Microfluidics and Nanofluidics (2021) 25:66
https://doi.org/10.1007/s10404-021-02466-3

RESEARCH PAPER

Cost-effective and rapid prototyping of PMMA microfluidic device via polymer-assisted bonding

Alper Baran Sözmen[1] · **Ahu Arslan Yildiz**[1]

Received: 20 April 2021 / Accepted: 24 June 2021 / Published online: 5 July 2021

Abstract

Microfluidic systems are relatively new technology field with a constant need of novel and practical manufacturing materials and methods. One of the main shortcomings of current methods is the inability to provide rapid bonding, with high bonding strength, and sound microchannel integrity. Herein we propose a novel method of assembly that overcomes the mentioned limitations. Polymer-assisted bonding is a novel, rapid, simple, and inexpensive method where a polymer is solubilized in a solvent and the constituted solution is used as a bonding agent. In this study, we combined this method with utilization of several phase-changing materials (PCMs) as channel-protective agents. Glauber's salt appeared to be more suitable as a channel-protective agent compared to rest of the salts that have been used in this study. Based on the bonding strength, quality analyses, leakage tests, and SEM imaging, the superior assisting bonding solvent was determined to be dichloromethane with a PMMA concentration of 2.5% (W/V). It showed a bonding strength of 23.794 MPa and a nearly non-visible bonding layer formation of 2.83 µm in width which is proved by SEM imaging. The said combination of PCM, solvent, and polymer concentration also showed success in leakage tests and an application of micro-droplet generator fabrication. The application was carried out to test the applicability of developed prototyping methodology, which resulted in conclusive outcomes as the droplet generator simulation run in COMSOL Multiphysics version 5.1 software. In conclusion, the developed fabrication method promises simple, rapid, and strong bonding with sharp and clear micro-channel engraving.

Keywords Microfluidics · Rapid prototyping · Microfabrication · Laser ablation · Micro-droplet generator

1 Introduction

Microfluidic devices become powerful tools for basic research and biomedical/clinical applications, since they provide rapid sample processing, excellent fluid handling and control, and ease of use. However, requirement of clean room facilities and sophisticated instruments are the main limitations for fabrication of microfluidics. Due to high demand, there is a need for the development of cost-effective and rapid prototyping methodologies, especially for point-of-care applications (Liu et al. 2021; Tsao and DeVoe 2008).

The very first microfluidic devices were mostly fabricated from silicone and glass, but alternative materials and fabrication methods are required due to expensive, long-lasting and inaccessible manufacturing methods, and fragile structure of glass (Mair et al. 2007). Therefore, polymer-based materials, such as Polymethylmethacrylate (PMMA), Polydimethylsiloxane (PDMS), SU-8 photoresist, Polycarbonate (PC) and Polystyrene, have been utilized because of their easy processability, durability, biocompatibility, and cost-effective features (Han et al. 2015; Zhang et al. 2014). PMMA is a commonly utilized thermoplastic polymer used in microfluidic systems due to its properties of transparency, chemical resistance, biocompatibility, and low cost. Recently, various PMMA bonding techniques have been reported, such as ultra violet (UV)-assisted bonding (Shinohara et al. 2007; Tsao et al. 2007) double-sided adhesive (DSA) (Zhu et al. 2006), solvent-bonding (Park et al. 2012), and thermal bonding (Rahbar et al. 2010). However, UV-assisted, DSA, and thermal bonding methods mostly result in reversible bonding with a low bonding strength, which is undesirable for sake of robustness and durability. Although, solvent-assisted chemical bonding is a good alternative to achieve high bonding strength and irreversible bonding, deformation of micro-channels due to solubilization of main

✉ Ahu Arslan Yildiz
ahuarslan@iyte.edu.tr

[1] Department of Bioengineering, Izmir Institute of Technology (IZTECH), 35430 Izmir, Turkey

material by organic solvents is a disadvantage. This deformation might be encountered as a collapse of the channel or fusing of channel walls due to solubilization especially at wider channel diameters (Thompson et al. 2015). The same issue is also seen in thermal bonding processes (Becker and Locascio 2002; Chu et al. 2015; Gan et al. 2011). Moreover, in case of solvent-bonding methods, channel deformation due to PMMA swelling is reported to take place and blocking of the channel due to solubilization can be encountered (Tran et al. 2013). In the case of PMMA bonding, microchannel deformation is generally prevented using a poor solvent of PMMA, such as ethanol, isopropyl alcohol, and their water mixtures, especially ethanol is widely used for its role both as a plasticiser and as a solvent of PMMA (Liga et al. 2016). Use of poor solvent causes little to no damage to microchannel integrity, but in some cases, these methods are reported to need higher bonding duration and show lower than desired bonding strength (Bamshad et al. 2016a; Zhang et al. 2014). The second most common strategy is to use strong PMMA solvents such as chlorinated organic solvents with a short exposure time, and then application of high pressure and heat. While it is possible to reach irreversible PMMA bonding via these techniques, the acquired bonding strength is much lower compared to the priors (De Marco et al. 2012; Ogilvie et al. 2010).

To overcome above-mentioned obstacles, here we propose a cost-effective and rapid prototyping methodology that combines a facile bonding method namely "polymer-assisted bonding" and use of inorganic salts as a phase-changing material (PCM) (Hintermüller and Jakoby 2019; Kelly et al. 2005; Koesdjojo et al. 2008; Lynh and Pin-Chuan 2018). In this study, we were motivated by the need of a new methodology, which provides high bonding strength of PMMA layers, and also protects the evenness of microfluidic channels.

For this purpose, CO_2 laser ablation on PMMA layer was carried out. Afterwards, protection of microchannel by inorganic PCMs was performed prior to polymer-assisted bonding that provides high bonding strength of PMMA layers. Sodium Sulfate Decahydrate, Magnesium Nitrate Hexahydrate, Magnesium Chloride Hexahydrate, and Aluminum Sulfate-18-Hydrate salts were used as PCM materials to investigate their capability. These salts were filled into the micro-channels in liquid phase above melting temperature and removed by water flow after fabrication. Sodium Sulfate Decahydrate, so called Glauber's salt, was found to be a superior protective agent compared to the rest due to its low melting point (32.4 °C) and slow hardening process. Characterization of the fabricated microfluidic chips was then carried out by leakage tests, bonding strength measurement, and SEM analysis. Lastly, as an application a T-junction microdroplet generator was simulated and fabricated by developed rapid microfabrication technique. The new bonding and fabrication technique proved to be simple and effective, providing easy control of parameters, such as diameter and channel structures; moreover, it did not need any external equipment, heating or cooling process, or unconventional solvent to remove PCMs.

2 Materials and methods

2.1 Materials

Following materials were used for microfabrication processes: $Na_2SO_4.10H_2O$ (Sigma Aldrich), $MgCl_2.6H_2O$ (LACHEMA), $Mg(NO_3)_2.6H_2O$ (Horasan Chemistry), and $Al_2(SO_4)_3.18\ H_2O$ (Sigma Aldrich), PMMA (Netpleksi), Dichloromethane (Sigma Aldrich), Chloroform (Merck), Toluene (Emsure).

2.2 Microfabrication and bonding

As depicted in Fig. 1, rapid prototyping process consisted of three main steps including: (i) design, (ii) microfabrication, and (iii) application. Designs of microfluidic chips were carried out by CorelDrawX6 software. During micromachining step, laser ablation parameters, such as speed and laser power, were examined to investigate the effects on channel width and depth. PMMA microfluidic chips were designed and fabricated as two layers. 3 mm thick PMMA sheets were used for fabrication of rectangular microfluidic chips (2×3 cm) using laser ablation method with a CO_2 laser cutter (Epilog Zing 16 Laser, USA; 40 watts of power at 100% power setting). After laser ablation, layers were cleaned by ethanol and deionized (DI) water, respectively, and were dried. Engraved channels were filled with melted PCM where four different types of salt hydrates, $Na_2SO_4.10H_2O$, $MgCl_2.6H_2O$, $Mg(NO_3)_2.6H_2O$, and $Al_2(SO_4)_3.18\ H_2O$ were used as channel-protective agents. PCMs were deposited into channels using a 10 µl micropipette and a ratio of 1 µl PCM per 1 mm^3 channel volume was used. After solidification of PCM, 100 µL of PMMA solution was applied (for a chip interface area of 4 cm^2) as a bonding agent on each PMMA surface, and two layers were combined quickly. Pressure was applied via clamps to bond layers and to remove air bubbles between two layers, and it was kept at room temperature until bonding is complete. As bonding agent varied PMMA solutions were utilized, 0.5, 1.0, 2.5 and 5% (W/V) PMMA in Dichloromethane (DCM), 0.5, 1.0, 2.5 and 5% (W/V) PMMA in Chloroform, and 2.5, 5.0, 7.5 and 10% (W/V) PMMA in toluene. After the bonding process, the PCM in the channels was liquefied and washed away for this purpose heated water was used. DI water at 60 °C was passed through channels for 15 min by a syringe pump (NE-300, The New Era Pump Systems, Inc., USA) to solubilize and to remove the residual PCM salt from the channels. Finally,

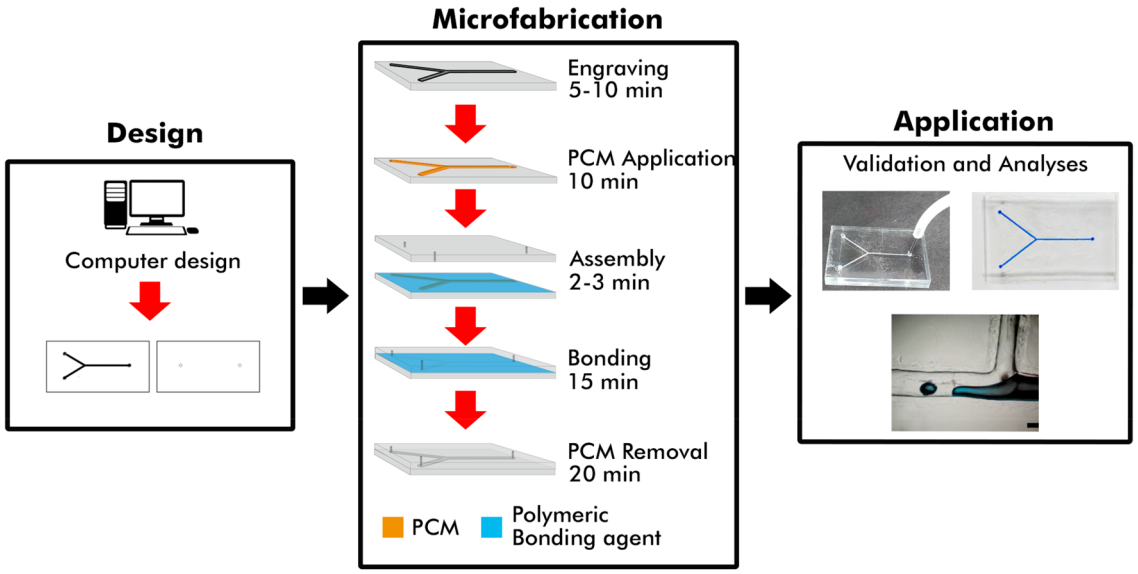

Fig. 1 Schematic representation for rapid prototyping of PMMA microfluidic chip

surface modification was done with solvent flow to acquire better smoothness and transparency in channel structure. DCM was applied through channels (10 ml/min) for duration of 120 s, and then pressurized air was applied for 120 s. All applications with DCM, Toluene, and Chloroform were handled under a chemical hood for safety purposes since their inhalation would cause acute metabolic and neurologic abnormalities.

2.3 Bonding strength, leakage and bonding analysis

Bonding strength of PMMA layers was investigated via tensile strength analyses, to observe effects of different solvents on bonding methodology. Bonding strength of DSA, DCM, chloroform, and toluene was compared against 0.5, 1.0, 2.5 and 5% (W/V) PMMA in DCM, 0.5, 1.0, 2.5 and 5% (W/V) PMMA in Chloroform, and 2.5, 5.0, 7.5 and 10% (W/V) PMMA in toluene. For bonding strength analysis, PMMA layers (70 mm × 20 mm × 2 mm) were fabricated through laser ablation. 100 µL of corresponding PMMA solution was added onto 4 cm^2 (20 mm × 20 mm) surface area of PMMA layers. Two PMMA layers were combined, and then clamp was used to apply pressure onto the bonded surface. The samples were held at room temperature until solvents evaporate and bonding complete. As a control group, only solvent-based bonding was used, where PMMA concentration was 0%. Measurements were carried out by Lloyd LR 30 K universal tensile testing machine. Two layers of PMMA were pulled apart with crosshead speed of 0.5 mm min^{-1}. Experiments were run in triplicates (Bamshad et al. 2016a). Later, bonding analyses of PMMA layers for cross section of channels were carried out by scanning electron microscopy (SEM, Philips XL 30S FEG). Finally, varied microfluidic chip patterns including I-shape, L-shape, Y-shape and S-shape were engraved on the PMMA sheets (20 mm × 30 mm) for leakage test. Leakage test was carried out using food dye solutions to investigate any possible leakage. To perform the leakage test, microfluidic chips with four different microchannel geometries were fabricated each 20 mm × 30 mm in size. Channel width and depth were fabricated to be 200 µm and 390 µm, respectively. Inlet and outlet holes were connected to silicone tubes (diameter: 1 mm) and utilizing a syringe pump (NE-300, The New Era Pump Systems, Inc., USA) water with blue food dye was passed though the micro-channels with a flow rate of 20 mL min^{-1}. Observation for any leakage was carried out visually.

2.4 Simulation and microfabrication of micro-droplet generator

As a model system, micro-droplet generator was fabricated to investigate the applicability of rapid prototyping methodology. First, simulation of the designed micro-droplet generator was done through COMSOL Multiphysics 5.1 software. Figure S1 shows the geometry of micro-droplet generator, where the horizontal channel is 300 µm in diameter and vertical channel is 200 µm; and it also shows regions and inlets, where red arrow indicates dispersed-phase (DP) inlet, green arrow indicates continuous-phase (CP) inlet, and the red line corresponds to initial interphase between two fluids. Flow rates were chosen to be 0.5 mL/h for dispersed phase and 10 mL/h for continuous phase. Mesh size was set to extremely fine, the geometry, materials, conditions, initial

values, interphases, and wall boundary conditions (non-slip) were set up and calculations were carried out. The number of degrees of freedom was 14,720, and each simulation took 6–8 h with less than 2 Gb of RAM. Figure 2 shows the geometry (2a), inputs (2b), and mesh grid (2c) used for the simulation.

Fabricated micro-droplet generator was tested for alginate micro-droplet formation. High oleic sunflower oil was used as CP, and aqueous solution of 1% alginate was used as DP. Blue food coloring was used to visualize alginate microdroplets. Produced alginate microdroplets were collected in a Petri dish, which consists of $CaCl_2$, and incubated until gelation is complete. The sizes of microdroplets for varied CP (5 and 10 ml/h) and DP (0.5, 1.0, and 2.0 ml /h) flow rates, and droplet frequency were examined. Droplet images were collected through light microscopy and high-speed camera during flow, and diameters were analyzed via ImageJ software.

3 Results and discussion

3.1 Micromachining process

Rapid prototyping of PMMA microfluidics involved following steps: (i) micromachining of channels via CO_2 laser ablation, (ii) protection of micro-channels by PCM, (iii) bonding of PCM protected PMMA layers, and (iv) removal of PCM from microchannels. First, to demonstrate the capability of CO_2 laser for the micromachining process two different modes; vector and raster modes were used. Here, the effect of different laser speeds on channel depth and structure for vector mode (laser power: 10%) and raster mode (laser power 100%) were investigated. To observe the channel depth and structures, cross-sectional SEM images of engraved PMMA surfaces were taken after laser ablation. (Fig. 3a, b). The channel depth was controlled by the laser speed, where raster mode created deeper channels compared to same speed range of vector mode due to higher energy density. It can be seen that channel depth decreases with increasing scanning speed. For microfabrication process, 30% speed with 100% power for raster mode was used; and for cutting, vector mode was used with 40% speed with 60% power.

Figure 3c shows light microscopy images of different microchannel patterns, where the channel width is ranging from 265 to 357 µm. It has to be noted that focused laser beam has 120 µm diameter, however, obtained channels were larger than the design due to partial melting of PMMA on the spot. When the laser ablation method is used for engraving laser moves in stepwise motion; therefore, perfectly smooth channels or structures cannot be obtained by this methodology. To obtain smooth channels and surface structures, channels were solvent-treated at post-processing step.

3.2 Bonding process

Bonding process is the most appealing part of the developed methodology. Here, polymer-assisted bonding technique is defined to overcome limitations of current methods, especially solvent-based bonding techniques. For bonding, PMMA polymer was solubilized in either in DCM, chloroform or toluene to obtain polymeric bonding agent, and applied onto PCM protected PMMA layers. PCMs were used to protect the micro-channels during bonding process and four different types of inorganic salts were investigated as possible channel protecting agents. Chemical formulations and melting points of each PCM are summarized in Table 1.

$Na_2SO_4.10H_2O$, namely Glauber's salt, appeared to be more suitable as a channel-protective agent compared to rest of the salts that have been used in this study. Due to its low melting temperature, it does not harden fast, which makes it easier to work with. Also, its solubility in water is quite high.

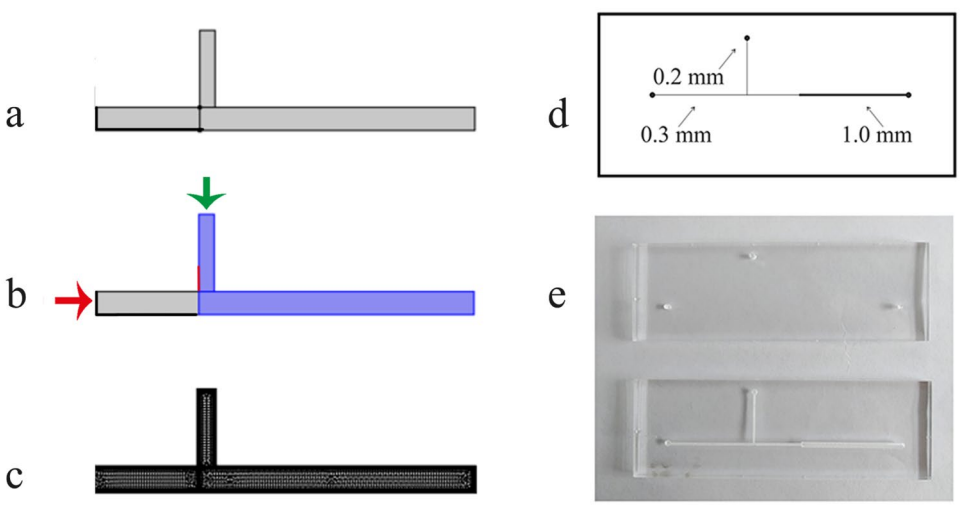

Fig. 2 **a** Geometry of simulated droplet fabrication chip. **b** Representation of continuous flow (green arrow) and dispersed flow (red arrow) inlets. **c** Mesh grid that's been used for simulation. **d** Dimensions of microdroplet formation microchip. **e** Fabricated microdroplet formation microchip (color figure online)

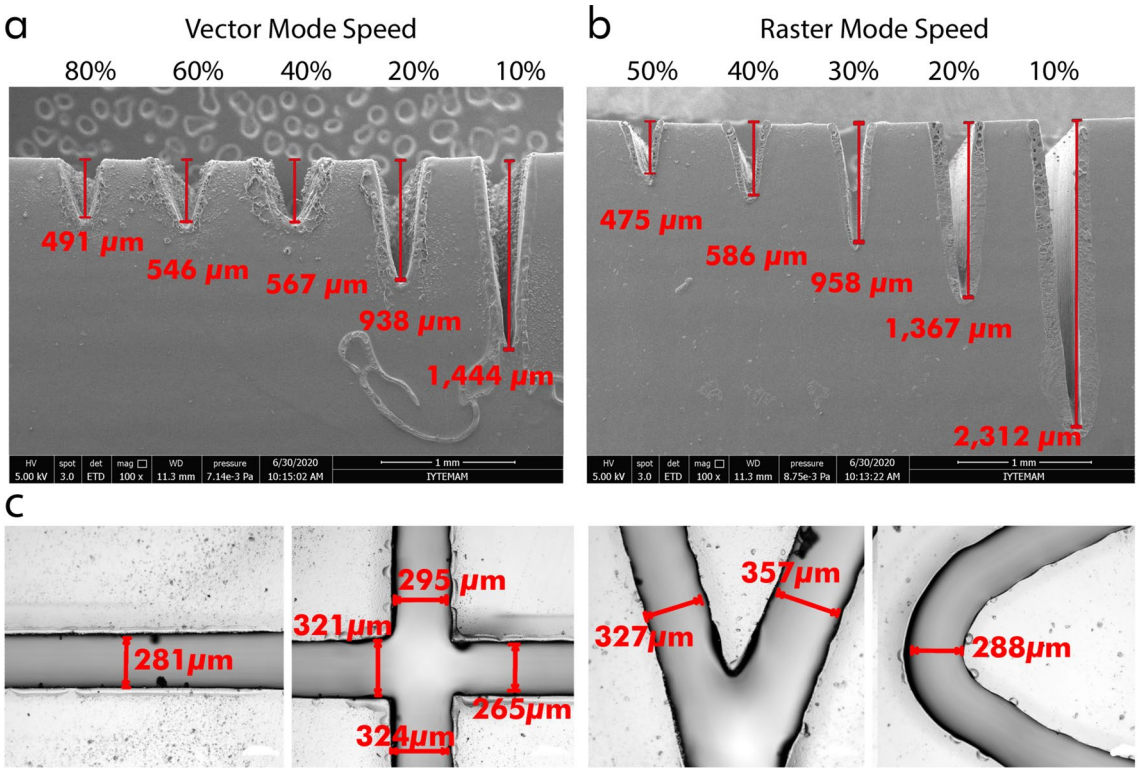

Fig. 3 PMMA surfaces that were engraved after laser cutting in micromachining process **a**, **b** SEM images of side view of channels: **a** Effect of different laser speed at vector mode, **b** Effect of different laser speed at raster mode; **c** Microscopy images of different patterns

Table 1 Names, chemical formulas and melting points of salts used as PCM

Inorganic salt hydrate PCM	Chemical formula	Melting point (°C)	Applicability for microfabrication
Sodium Sulfate Decahydrate (Glauber's salt)	$Na_2SO_4 \cdot 10H_2O$	32.4	Excellent
Magnesium Nitrate Hexahydrate	$Mg(NO_3)_2 \cdot 6H_2O$	89.0	Mediocre
Magnesium Chloride Hexahydrate	$MgCl_2 \cdot 6H_2O$	117.0	Poor
Aluminum Sulfate-18-Hydrate	$Al_2(SO_4)_3 \cdot 18\ H_2O$	90.0	Poor

This resulted in no-salt residuals in micro-channels after bonding and PCM removal process where salt residues were obtained for other PCMs used during this study either due to their higher melting temperatures and/or lower solubilities in water. Rest of the salts had higher melting points and they possessed faster solidifying speeds, which was not desirable. Therefore, they were not convenient for complete protection of channels, and mostly resulted in deformations of channels during bonding and PCM removal. $Mg(NO_3)_2.6H_2O$ was also an applicable PCM; where it turned into solid phase faster than Glauber's salt but slower than other salts. Overall, Glauber's salt was much easier to work with and the longest microchannel that was processed with above-mentioned PCMs was 27.2 mm in length.

3.3 Bonding strength and bonding quality analysis

Bonding strength and reversibility of bonding were evaluated for polymeric bonding agents where varied concentrations of PMMA solutions obtained through different solvents. Also, the bonding strength of these polymeric bonding agents was compared with DSA. To examine the bonding strength and reversibility, tensile strength test was performed for each bonding agent. As given in Fig. 4, highest bonding strength was obtained for DCM solubilized bonding agents that is 23.794 ± 2.7 MPa. Bonding strength of DCM, chloroform, toluene and double-side adhesive without the solubilization of PMMA as a bonging agent were obtained as 14.8 ± 2.4 MPa, 10.9 ± 3.7 MPa, 13.8 ± 3.5 MPa and 9.5 ± 1.0 MPa, respectively. Compared to solvent-bonding group, where 0% PMMA was used, DCM solubilized

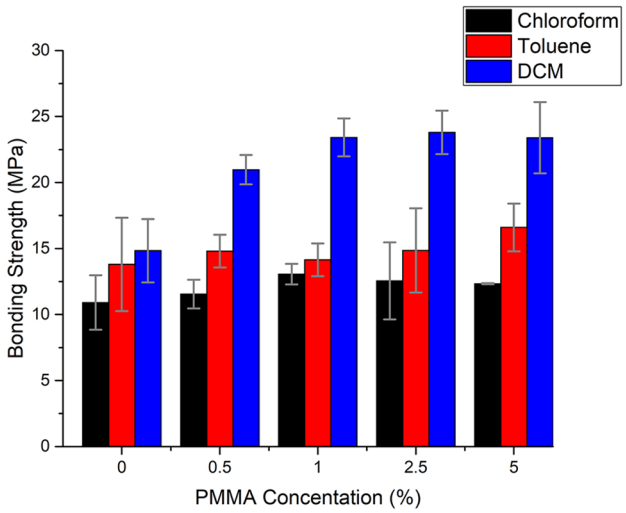

Fig. 4 Effects of organic solvents with different PMMA concentrations on bonding strength of PMMA layers. Effect of PMMA concentration and solvent type on bonding strength between two layers

bonding agents provided improved bonding strength. DCM solubilized bonding agent provides higher bonding strength than chloroform and toluene because of its solubility properties. In literature, PMMA solvents, such as chloride compounds, chloroform and alcohols, as well as different bonding techniques have been reported under solvent-bonding (Mair et al. 2007; Tsao and DeVoe 2008; Umbrecht et al. 2009; Zhang et al. 2014). Our results revealed that polymer-assisted bonding provided higher strength and better bonding than larger part of those methods as shown Table 2.

DCM readily showed higher modulus compared to toluene in literature and this is explained by its higher affinity to PMMA (Fashandi and Karimi 2014). This affinity is further investigated by utilizing "Hansen Solubility Space", determination of the maximum distance between solvent and solute in the "solubility" space (*D* value). Fashandi and Karimi calculated the *D* values of PMMA-Toluen (10.7) and PMMA-DCM (4.54) to compare their bonding affinity and showed that there is a relation between the D value and solvent-polymer interaction; the lower the *D* value the more affinity of a solvent towards a solute. Herein the *D* value is calculated for chloroform and PMMA using the parameters taken from literature to be 7.78 (Bordes et al. 2010; Lara et al. 2016). The *D* value of DCM is apparently the lowest (4.54) among the used solvents in this study which supports the Solubility Space claim by Bordes et al. and Fashandi and Karimi and provides a grounding for its superior bonding strength test results.

For all of the polymeric bonding agents, irreversible bonding was obtained; where PMMA substrates were detached only when they are broken. On the other hand, reversible bonding was obtained for DSA where PMMA substrates were detached without physical damage. Effect of the bonding was investigated by analyzing bonding area of completed microfluidic chip, which was bonded with the help of PCM. Here, only Glauber's salt was used as a PCM because of its convenience. Figure 5a demonstrates the SEM analysis for cross section of fabricated microfluidic chips when different concentrations (0%, 0.5%, 1%, and 2.5% PMMA in DCM) of PMMA bonding agent were applied. Continuous line on cross-sectional images indicates two PMMA layers fused well during bonding process. As PMMA concentration increased, distinctions between two layers were decreased. Sample that has been bonded with no PMMA in its boning agent showed a boundary layer of 33.65 µm, where the sample with 2.5% PMMA dissolved in its bonding agent showed 2.83 µm. There was a clear decrease in observed boundary breadth showing irreversible and high-quality bonding is achieved. On the contrary, a thick bonding layer formation is observed when solvent-bonding was done using only DCM, which affects the bonding quality and strength negatively. It is a well known fact that applying solvent directly on substrate causes dissolution of substrate material, therefore defects may occur on the bonding surface and substrate itself. However, in the developed methodology, polymeric bonding agent provided a homogeneous thin film layer for easy fusion of two PMMA layers while

Table 2 Comparison of the highest bonding strength values acquired in tensile strength test with related studies

	Solvent	Bond strength (MPa)
This work	DCM	23.8 ± 2.4
	Chloroform	13.1 ± 3.7
	Toluene	16.6 ± 3.5
(Umbrecht et al. 2009)	Ethylene glycol dimethacrylate	3.10
(Brown et al. 2006)	Solution of methyl sulfoxide, water and methanol	5.50
(Hsu and Chen 2007)	Isopropanol	4.02
(Zhang et al. 2014)	Ethanol/Chloroform (5:1 v/v)	7.12
(Ogilvie et al. 2010)	Chloroform	3.10

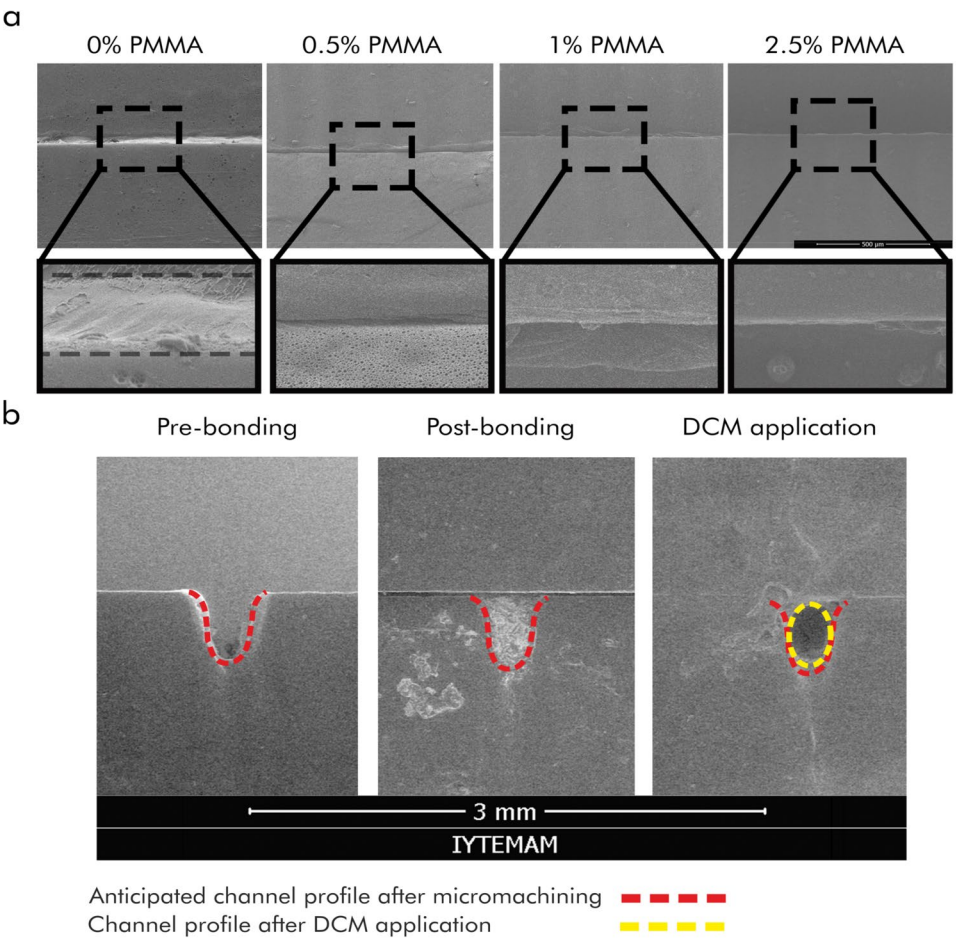

Fig. 5 **a** Side view SEM images of microchips after fabricated using DCM with different PMMA concentrations, bonding layers can be observed between the dashed lines. **b** Step-by-step SEM images of rapid prototyping process, after micromachining, after PCM application and bonding, and after removal of PCM via DCM

protecting the integrity of the substrate and preventing dissolution. In this manner, obtained results correlate with bonding strength analysis, which are shown in Fig. 3.

Figure 5b shows profile of the micro-channels, comparing microchannel profiles right after micromachining and after DCM application. Channel profile after micromachining is denoted by dashed red line and profile acquired after DCM application is highlighted with yellow dashed line. It can be seen in the figure that produced (depth: 389.6 µm; width: 271.3 µm) and anticipated (depth: 417.4 µm; width: 274.8 µm) microchannel profiles are similar in terms of depth and width. Where depth values deviated 6.67% from first anticipation, width values deviated 1.27%; both presumed acceptable results compared to previous literature (Prakash and Kumar 2015; Sun et al. 2006). Moreover microchannels preserved integrity, showing that the developed prototyping method is promising. Overall, circular channel structure has been achieved without a thick bonding layer between two PMMA layers, and with good channel integrity which are essential for producing complex microchannel structures for areas, such as tissue engineering, lab on a chip systems, or proteomics (He et al. 2017; Song et al. 2010; Thompson et al. 2015).

To investigate the bonding efficiency and sealing of microfluidic chip, chips with four distinct geometries were fabricated. Microchip sizes were 20 mm × 30 mm with channel width of 200 µm and channel depth of 389.6 ± 4.95 µm. All bonding was carried out with Glauber's salt as the channel-protective agent and 2.5% PMMA in DCM as the bonding agent. Leakage test was performed via liquid flow where the flow rate was adjusted to 20 mL min^{-1} (Velocity: 3.703 m/s; Pressure 40.867 kPa) with the longest microchannel length of 27.2 mm. As given in Fig. 6, different microfluidic chip designs fabricated by developed methodology and blue-colored dye solution was used for leakage test. The physical durability of the different designs was evaluated for all polymeric bonding agent concentrations. None of the patterns showed any leakage, exhibiting success of bonding between layers and channel integrity.

Although parameters of leakage tests highly depend on the material used to fabricate microfluidic chips, and microchannel size and shape. Considering the microchannel sizes and microchip fabrication material, the results acquired in this study are comparable with recent studies (Lin et al. 2007; Rahbar et al. 2010; Song and Park 2017; Tan et al. 2010; Tran et al. 2013; Zhang et al. 2014; Zhu et al. 2006).

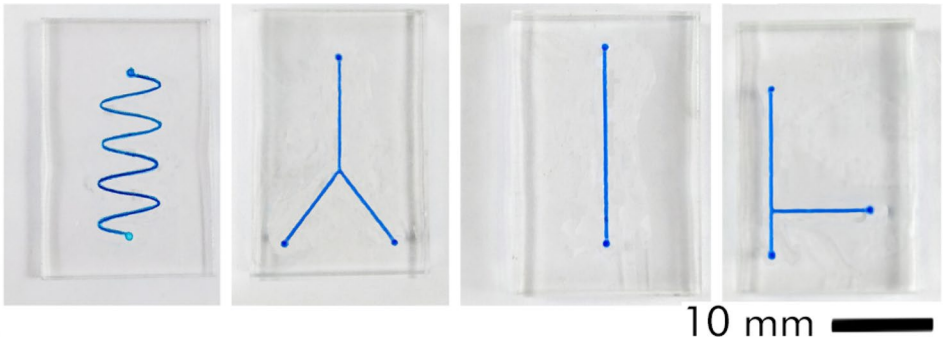

Fig. 6 Leakage test of microfluidic chips with different channel patterns

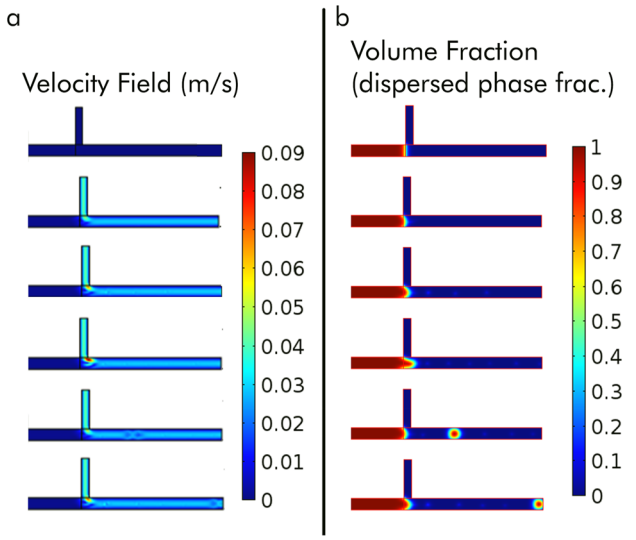

Fig. 7 **a** Velocity field and **b** Volume Fraction plots of droplet formation platform with increasing time (0: 0.5 s; with 0.01 s increments)

Considering the flow rate used during the test, it is comparable to a recent study by Ramshad et al., whom tested microchips (Microchannel size: 145 µm × 600 µm) with flow rates between 10 µl min^{-1} and 35.7 µl min^{-1} where the first leakage was observed (Bamshad et al. 2016b). Overall, the developed method succeeded in leakage tests applied in this study.

3.4 Simulation and application: microdroplet generator

To demonstrate the analytical performance of the fabricated microfluidic device, a T-junction microdroplet generator was designed and employed. First, simulations were carried out by steady state Navier–Stokes equation or incompressible Newtonian fluids. As shown in Fig. 7a, velocity showed a uniform distribution along the microfluidic channel and a ~ 150 droplet/min droplet formation frequency was calculated for flow rates of dispersed-phase (red) flow rate: 0.5 mL/h, continues phase (blue) flow rate: 10 mL/h. Figure 7a, b shows simulated contours of velocity field and volume fraction during droplet formation, respectively. The droplet started to form below channel intersection, as droplet grew a neck formation was observed which decreased in size with time and droplet detached with a final diameter of nearly 150 µm. Maximum velocity in channel was observed before droplet formation, which correlates with pressure field. Pressure in inlet channels was around 60 Pa until the neck formation started. With neck formation continuous-phase inlet pressure increased to 90 Pa and dispersed-phase inlet pressure to 80 Pa, then decreased back to 60 Pa with detachment of droplet, in concurrence with velocity gradient maximum inlet pressure was observed right before detachment of the droplet. The pressures and velocities increased again after detachment, as an effect of the reorientation of the dispersed phase remaining at the channel opening. The pressure field at intersection of channels can be considered the main induction of droplet formation other elements that induce the formation are continuous-phase flow and the shear from cross flow which also cause the circulatory movement of droplets. This circulation has a higher velocity than the continuous phase behind the drop; this difference leads to a shear stress between droplet and surrounding flow that is centralized at the center of the droplet which correlates with previous literature (Antar and El-Shaarawi 2004).This shear results in promoting the droplet detachment and also affects the size and circularity of the droplets. Simulation results showed that with increased inlet pressure it is possible to reach higher droplet sizes and also pressure inside and around the droplet affects the outlet pressure and velocity.

A T-junction micro-droplet generator was designed (Figure 2-d) and fabricated (Figure 2-e) to test the applicability of developed prototyping methodology. Dimensions of the used platform and micro-fabricated PMMA layers can be seen in Fig. 2d. After microfabrication process channels were protected with Glauber's salt, then two PMMA layers were bound to each other via developed polymer-based bonding methodology, and finally inlet/outlet tubings were connected.

Figure 8a shows the formation of microdroplet in the continuous phase, frame by frame. As simulated before, neck

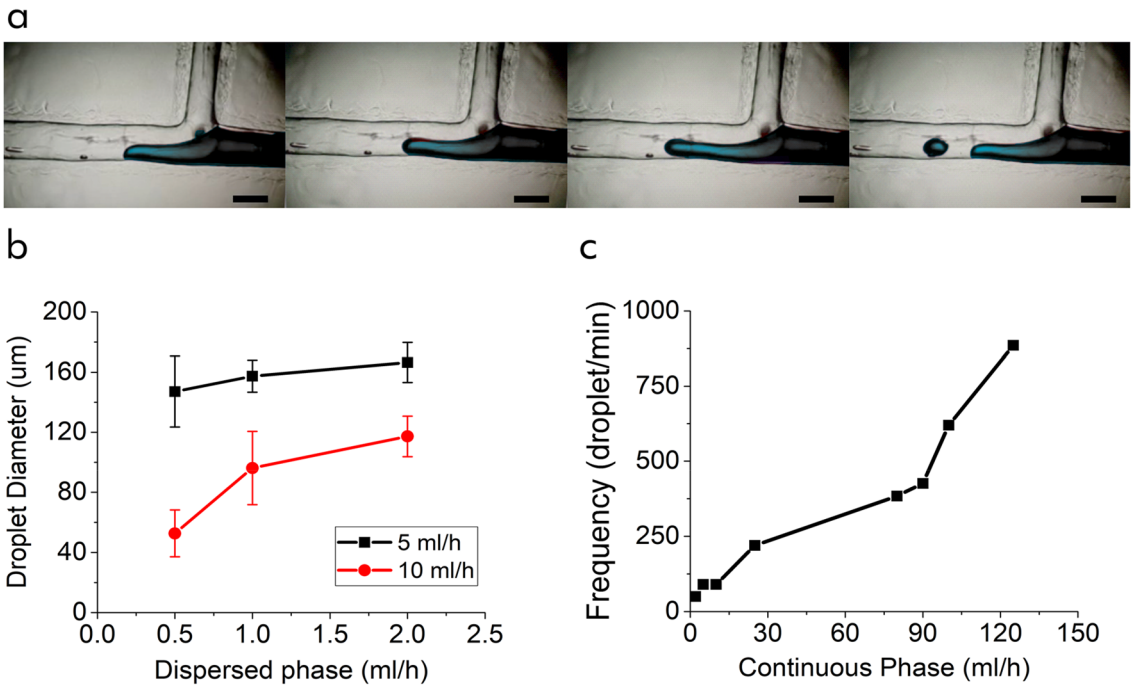

Fig. 8 **a** Images of droplet formation in microdroplet-on-a-chip system. Dispersed Phase (blue) Flow rate: 1 ml/h, Continues phase Flow rate: 5 ml/h. **b** Droplet size relationship with flow rates of dispersed and continuous phases. **c** Continuous phase flow rate and droplet formation frequency relationship. All results are mean values or figures representing droplets generated by respective parameters. Experiments were run in triplicates and mean droplet diameters were calculated using diameter values of 18 randomly picked droplets of each parameter (color figure online)

formation and detachment of the droplet can be observed in detail. This study showed that droplet size is changing with varying flow rates of both continuous and dispersed phases (Fig. 8b). When the continuous-phase flow rate was held constant and dispersed-phase flow rate was increased, a slight increase in the droplet size was monitored, also when dispersed-phase flow rate was held constant and flow rate of continuous phase was increased, droplet sizes also increased significantly. However, the effect of dispersed-phase flow rate was insignificant at higher continuous-phase flow rates. Flow rate changes also affected droplet formation frequency; with increasing continuous-phase flow rate droplet formation frequency increased too. Figure 8c shows the relation between flow rate and droplet frequency; a semi-linear relationship between them was observed.

4 Conclusion

In this study, a new polymer-assisted bonding methodology with PCM utilization was developed, which provides high bonding strength for PMMA layers and also protects the evenness of microfluidic channels. Effects of different solvents and their PMMA solutions on bonding strength and quality were investigated during the study, where 2.5% PMMA in DCM provided the highest bonding strength. Undesired effects of bonding agents on channel integrity were minimized using PCMs as channel-protective agents. Glauber's salt had given the most promising results with its relatively lower melting point and its higher solubility in water. It has been shown that this salt can be used as a channel-protective agent in micro-channels with diameters as low as 120 µm in combination with a polymer-assisted bonding method. Besides, it has been confirmed that developed methodology is applicable to different channel geometries preserving said features. Finally, a T-junction micro-droplet generator was fabricated to test the applicability of the rapid prototyping method. Results of the application were then compared with the simulation results obtained from COMSOL Multiphysics version 5.1 software. Results of the application and simulation were coherent. In conclusion, developed microfluidic chip fabrication methodology (i) is simple and rapid, (ii) provides high bonding strength, and (iii) protects microchannel integrity. Overall, the whole fabrication process took less than an hour and it was applicable to even complicated microfluidic chip designs.

Acknowledgements The authors acknowledge Izmir Institute of Technology Center for Materials Research (IZTECH-MAM) for the

instrumental facilities provided to accomplish this work. We thank to Dr. Ümit Tayfun for tensile strength analysis. We would like to also thank Nida Demircak and Nihan Atak for their feedback and fruitful discussions.

References

Antar MA, El-Shaarawi MAI (2004) Simultaneous effect of rotation and natural convection on the flow about a liquid sphere. Heat Mass Transf 40(5):393–399. https://doi.org/10.1007/s00231-003-0429-9

Bamshad A, Nikfarjam A, Khaleghi H (2016b) A new simple and fast thermally-solvent assisted method to bond PMMA–PMMA in micro-fluidics devices. J Micromech Microeng. https://doi.org/10.1088/0960-1317/26/6/065017

Bamshad A, Nikfarjam A, Khaleghi H (2016a) A new simple and fast thermally-solvent assisted method to bond PMMA–PMMA in micro-fluidics devices. J Micromech Microeng 26(6):065017. https://doi.org/10.1088/0960-1317/26/6/065017

Becker H, Locascio LE (2002) Polymer microfluidic devices. Talanta, 56

Bordes C, Freville V, Ruffin E, Marote P, Gauvrit JY, Briancon S, Lanteri P (2010) Determination of poly(epsilon-caprolactone) solubility parameters: application to solvent substitution in a microencapsulation process. Int J Pharm 383(1–2):236–243. https://doi.org/10.1016/j.ijpharm.2009.09.023

Brown L, Koerner T, Horton JH, Oleschuk RD (2006) Fabrication and characterization of poly(methylmethacrylate) microfluidic devices bonded using surface modifications and solvents. Lab Chip 6(1):66–73. https://doi.org/10.1039/b512179e

Chu C, Jiang B, Zhu L, Jiang F (2015) A process analysis for microchannel deformation and bonding strength by in-mold bonding of microfluidic chips. J Polym Eng 35(3):267–275. https://doi.org/10.1515/polyeng-2013-0092

De Marco C, Eaton SM, Martinez-Vazquez R, Rampini S, Cerullo G, Levi M, Osellame R (2012) Solvent vapor treatment controls surface wettability in PMMA femtosecond-laser-ablated microchannels. Microfluid Nanofluid 14(1–2):171–176. https://doi.org/10.1007/s10404-012-1035-2

Fashandi H, Karimi M (2014) Influence of solvent/polymer interaction on miscibility of PMMA/PCL blend: thermal analysis approach. J Text Polym 2(2)

Gan Z, Zhang L, Chen G (2011) Solvent bonding of poly(methyl methacrylate) microfluidic chip using phase-changing agar hydrogel as a sacrificial layer. Electrophoresis 32(23):3319–3323. https://doi.org/10.1002/elps.201100436

Han X, Liu X, Tian L, Zhang H, Mao Z-G (2015) A non-photolithography fabrication for a microfluidic chip based on PMMA polymer. Machines 3(2):107–122. https://doi.org/10.3390/machines3020107

He R, Yunus D, Uhl C, Shi W, Sohrabi S, Liu Y (2017) Fabrication of circular microfluidic channels through grayscale dual-projection lithography. Microfluid Nanofluid. https://doi.org/10.1007/s10404-017-1851-5

Hintermüller MA, Jakoby B (2019) Lab-scale prototyping of polymer based microfluidic devices using gallium as phase-changing sacrificial material. Microelectron Eng 211:50–54. https://doi.org/10.1016/j.mee.2019.03.025

Hsu YC, Chen TY (2007) Applying Taguchi methods for solvent-assisted PMMA bonding technique for static and dynamic micro-TAS devices. Biomed Microdevices 9(4):513–522. https://doi.org/10.1007/s10544-007-9059-1

Kelly RT, Pan T, Woolley AT (2005) Phase-changing sacrificial materials for solvent bonding of high-performance polymeric capillary electrophoresis microchips. Anal Chem 77(11):3536–3541

Koesdjojo MT, Tennico YH, Rundel JT, Remcho VT (2008) Two-stage polymer embossing of co-planar microfluidic features for microfluidic devices. Sens Actuatorss B Chem 131(2):692–697. https://doi.org/10.1016/j.snb.2008.01.008

Lara J, Zimmermann F, Robert R, Drolet D, Hansen CM, Monta N (2016) The use of the Hansen solubility parameters in the selection of protective polymeric materials resistant to chemicals. Int J Curr Res 9(3)

Liga A, Morton JAS, Kersaudy-Kerhoas M (2016) Safe and cost-effective rapid-prototyping of multilayer PMMA microfluidic devices. Microfluid Nanofluid. https://doi.org/10.1007/s10404-016-1823-1

Lin C, Chao C, Lan C (2007) Low azeotropic solvent for bonding of PMMA microfluidic devices. Sens Actuators B Chem 121(2):698–705. https://doi.org/10.1016/j.snb.2006.04.086

Liu P, Lv Z, Sun B, Gao Y, Qi W, Xu Y, Li S (2021) A universal bonding method for preparation of microfluidic biosensor. Microfluid Nanofluid. https://doi.org/10.1007/s10404-021-02445-8

Lynh HD, Pin-Chuan C (2018) Novel solvent bonding method for creation of a three-dimensional, non-planar, hybrid PLA/PMMA microfluidic chip. Sens Actuators A 280:350–358. https://doi.org/10.1016/j.sna.2018.08.002

Mair DA, Rolandi M, Snauko M, Noroski R, Svec F, Frechet JM (2007) Room-temperature bonding for plastic high-pressure microfluidic chips. Anal Chem 79(13):5097–5102. https://doi.org/10.1021/ac070220w

Ogilvie IRG, Sieben VJ, Floquet CFA, Zmijan R, Mowlem MC, Morgan H (2010) Solvent processing of pmma and coc chips for bonding devices with optical quality surfaces. In: Paper presented at the 14th International Conference on Miniaturized Systems for Chemistry and Life Sciences, Groningen, The Netherlands

Park T, Song IH, Park DS, You BH, Murphy MC (2012) Thermoplastic fusion bonding using a pressure-assisted boiling point control system. Lab Chip 12(16):2799–2802. https://doi.org/10.1039/c2lc40252a

Prakash S, Kumar S (2015) Profile and depth prediction in single-pass and two-pass CO_2 laser microchanneling processes. J Micromech Microeng. https://doi.org/10.1088/0960-1317/25/3/035010

Rahbar M, Chhina S, Sameoto D, Parameswaran M (2010) Microwave-induced, thermally assisted solvent bonding for low-cost PMMA microfluidic devices. J Micromech Microeng. https://doi.org/10.1088/0960-1317/20/1/015026

Shinohara H, Mizuno J, Shoji S (2007) Low-temperature direct bonding of poly(methyl methacrylate) for polymer microchips. IEEJ Trans Electr Electron Eng 2(3):301–306. https://doi.org/10.1002/tee.20157

Song IH, Park T (2017) PMMA Solution Assisted Room Temperature Bonding for PMMA(-)PC Hybrid Devices. Micromachines (basel). https://doi.org/10.3390/mi8090284

Song S-H, Lee C-K, Kim T-J, Shin I-C, Jun S-C, Jung H-I (2010) A rapid and simple fabrication method for 3-dimensional circular microfluidic channel using metal wire removal process. Microfluid Nanofluid 9(2–3):533–540. https://doi.org/10.1007/s10404-010-0570-y

Sun Y, Kwok YC, Nguyen N-T (2006) Low-pressure, high-temperature thermal bonding of polymeric microfluidic devices and their applications for electrophoretic separation. J Micromech Microeng 16(8):1681–1688. https://doi.org/10.1088/0960-1317/16/8/033

Tan HY, Loke WK, Nguyen N-T (2010) A reliable method for bonding polydimethylsiloxane (PDMS) to polymethylmethacrylate (PMMA) and its application in micropumps. Sens Actuators B Chem 151(1):133–139. https://doi.org/10.1016/j.snb.2010.09.035

Thompson BL, Ouyang Y, Duarte GR, Carrilho E, Krauss ST, Landers JP (2015) Inexpensive, rapid prototyping of microfluidic devices using overhead transparencies and a laser print, cut and laminate fabrication method. Nat Protoc 10(6):875–886. https://doi.org/10.1038/nprot.2015.051

Tran HH, Wu W, Lee NY (2013) Ethanol and UV-assisted instantaneous bonding of PMMA assemblies and tuning in bonding reversibility. Sens Actuators B Chem 181:955–962. https://doi.org/10.1016/j.snb.2012.11.060

Tsao C-W, DeVoe DL (2008) Bonding of thermoplastic polymer microfluidics. Microfluid Nanofluid 6(1):1–16. https://doi.org/10.1007/s10404-008-0361-x

Tsao CW, Hromada L, Liu J, Kumar P, DeVoe DL (2007) Low temperature bonding of PMMA and COC microfluidic substrates using UV/ozone surface treatment. Lab Chip 7(4):499–505. https://doi.org/10.1039/b618901f

Umbrecht F, Müller D, Gattiker F, Boutry CM, Neuenschwander J, Sennhauser U, Hierold C (2009) Solvent assisted bonding of polymethylmethacrylate: Characterization using the response surface methodology. Sens Actuators A 156(1):121–128. https://doi.org/10.1016/j.sna.2009.03.028

Zhang H, Liu X, Li T, Han X (2014) Miscible organic solvents soak bonding method use in a PMMA multilayer microfluidic device. Micromachines 5(4):1416–1428. https://doi.org/10.3390/mi5041416

Zhu X, Liu G, Guo Y, Tian Y (2006) Study of PMMA thermal bonding. Microsyst Technol 13(3–4):403–407. https://doi.org/10.1007/s00542-006-0224-x